5350 *Inorg. Chem.* **2009**, *48*, 5350–5360
DOI: 10.1021/ic9003005

Inorganic Chemistry
Article

The Sulfate Coordination of Np(IV), Np(V), and Np(VI) in Aqueous Solution

Christoph Hennig,*,† Atsushi Ikeda-Ohno,†,‡ Satoru Tsushima,† and Andreas C. Scheinost†

†*Institute of Radiochemistry, Forschungszentrum Dresden-Rossendorf, P.O. Box 510119, 01314 Dresden, Germany, and* ‡*Synchrotron Radiation Research Center (Spring-8), Japan Atomic Energy Agency, Kouto 1-1-1, Sayo-cho, Sayo-gun, 679-5148 Hyogo-ken, Japan*

Received February 13, 2009

The coordination and redox behavior of Np(IV), Np(V), and Np(VI) sulfate in aqueous solution were investigated by Np L_3-edge extended X-ray absorption fine structure (EXAFS) spectroscopy, cyclic voltammetry, and density functional theory (DFT) calculations. The sulfate coordination mode, that is, monodentate versus bidentate, was determined by using neptunium−sulfur distances R_{Np-S} and coordination numbers N_S obtained by EXAFS spectroscopy. Np(VI) is coordinated by sulfate in the bidentate ($R_{Np-S} = 3.12 \pm 0.02$ Å) and monodentate ($R_{Np-S} = 3.61 \pm 0.02$ Å) modes at a low sulfate concentration of $[SO_4^{2-}]/[NpO_2^{2+}] = 1$. At higher $[SO_4^{2-}]/[NpO_2^{2+}]$ ratios, bidentate coordination prevails. Approximately two bidentate sulfate groups are coordinated to Np(VI) with 2.0 M SO_4^{2-} and at pH 1.1. Np(V) is coordinated by sulfate in the bidentate ($R_{Np-S} = 3.16 \pm 0.02$ Å) and monodentate ($R_{Np-S} = 3.67 \pm 0.02$ Å) modes. However, sulfate coordination is less pronounced and does not exceed one SO_4^{2-} per Np(V) with 2.0 M SO_4^{2-}. The redox reaction between the Np(VI)/Np(V) couple can be basically categorized as quasi-reversible. It becomes a more irreversible character at high sulfate concentrations due to structural rearrangement of the sulfate ligands. Finally, Np(IV) also shows bidentate ($R_{Np-S} = 3.06 \pm 0.02$ Å) and monodentate ($R_{Np-S} = 3.78 \pm 0.02$ Å) coordination modes. The sulfate coordination increases with an increasing $[SO_4^{2-}]/[Np^{4+}]$ ratio. A comparison of other tetravalent actinides shows that the monodentate sulfate coordination decreases whereas the bidentate coordination increases along the series Th(IV)−U(IV)−Np(IV). This trend was studied by DFT calculations and is discussed in terms of solvation energy and increasing number of unpaired electrons.

Introduction

Neptunium isotopes occur naturally in uranium ore in trace amounts, since ^{237}Np and ^{239}Np are generated from ^{238}U and ^{235}U by neutron capture from spontaneous fission and by spallation reactions induced by cosmic rays.[1] Several Np isotopes occur as a byproduct in nuclear reactors, but only ^{237}Np accumulates over the reactor operation time and later in the nuclear waste repository to large quantities because of its long half-life ($T_{1/2} = 2.144 \times 10^6$ years). Neptunium is considered one of the most problematic actinide elements for waste storage due to its relatively high solubility in aqueous solution.[2] The geochemical behavior depends strongly on the valence state. Neptunium can occur in solution in the oxidation states III, IV, V, VI, and VII. The stability of the oxidation state is affected by the acidity of the solution; that is, the reduction potentials largely differ depending on the pH.[3] Np(V) is considered mobile in the environment because of its relatively high solubility and low sorption capacity by minerals.[4] In contrast, Np(IV) forms strong complexes and shows significant interactions with soil constituents. The environmental behavior of Np(VI) is similar to that of U(VI)—characterized by high solubility in aqueous solution and high stability under oxidizing conditions. Np(III) and Np(VII) are not likely to occur under environmental conditions.

Sulfate and hydrogen sulfate anions occur in natural waters in significant concentrations and are able to form moderately strong complexes with neptunium. As a consequence, sulfate complexation may play an important role in the migration of neptunium from nuclear waste repositories. Thermodynamic data in aqueous solution are reported for Np(IV), Np(V), and Np(VI) sulfate.[5] The data were obtained

*To whom the correspondence should be addressed. E-mail: hennig@esrf.fr.

(1) Yoshida, Z.; Johnson, S. G.; Kimura, T.; Krsul, J. R. Neptunium. In *The Chemistry of the Actinide and Transactinide Elements*; Morss, L. R., Edelstein, N. M., Fuger, J., Eds.; Springer: Heidelberg, Germany, **2005**; Vol. *2*, p 669.

(2) Viswanathan, H. S.; Robinson, B. A.; Valocchi, A. J.; Triay, I. R. *J. Hydrol.* **1998**, *209*, 251.

(3) Katz, J. J.; Seaborg, G. T.; Morss, L. R. *The Chemistry of the Actinide Elements*; Chapman and Hall: London, **1986**; Vol. *1*, pp 469−487.

(4) Kaszuba, J. P.; Runde, W. H. *Environ. Sci. Technol.* **1999**, *33*, 4427.

(5) (a) Lemire, J. L.; Fuger, L.; Nitsche, H.; Potter, P.; Rand, M. H.; Rydberg, J.; Spahiu, K.; Sullivan, J. C.; Ullman, W. J.; Vitorge, P.; Wanner, H. *Chemical Thermodynamics of Neptunium and Plutonium*; Elsevier Science Publishers: Amsterdam, **2001**.(b) Guillaumont, R. et al. *Update on the Chemical Thermodynamics of Uranium, Neptunium, Plutonium, Americium and Technetium* Mompean, F. J., Illemassene, M., Domenech-Orti, C., Ben Said, K., Eds.; Elsevier Science Publishers: Amsterdam, **2003**.

Published on Web 05/14/2009

in acidic solutions where HSO_4^- dominates over SO_4^{2-}. From a thermodynamic point of view, it is assumed that both HSO_4^- and SO_4^{2-} form complexes with Np.[6,7] The examined equilibrium constants at zero ionic strength are listed in the Supporting Information, Table S1. These data suggest that sulfate complexation is strongest for Np(IV), intermediate for Np(VI), and weakest for Np(V). The equilibrium constants for Np(IV) were generally determined in strong acidic media to avoid interference with hydrolysis. The coordination geometry of neptunium depends on the oxidation state: Np(III) and Np(IV) are spherically coordinated ions, Np(V) and Np(VI) form the linear trans-dioxo cations NpO_2^+ and NpO_2^{2+}, and Np(VII) forms the tetraoxo cation NpO_4^-.[8−10] The early pentavalent actinides show a particular disproportionation behavior. Np(V) does not follow the disproportion mechanism of U(V) and Pu(V), as studied recently by quantum chemical calculations.[11]

The current knowledge on the coordination of neptunium sulfates is based almost exclusively on diffraction studies in the solid state. The deduction of aqueous coordination from solid coordination may be misleading, because it is known that the solution species may undergo a ligand rearrangement during the crystallization process.[12] Therefore, the direct determination of the coordination in solution is mandatory. Among several techniques suited to study the structure of aqueous complexes, extended X-ray absorption fine structure (EXAFS) spectroscopy has the advantage that the environment of the excited atom is selectively probed, resulting in a higher sensitivity. A comprehensive overview of the results obtained with Np L_3-edge EXAFS spectroscopy, given by Antonio and Soderholm,[13] shows that EXAFS studies of neptunium sulfates are scarce. To the best of our knowledge, there exists, up to now, only one EXAFS measurement of Np(IV) in 0.1 M HNO_3/2.0 M H_2SO_4, suggesting an average of 2.2 sulfate groups in bidentate coordination mode.[14] Other actinides in oxidation state IV, like Th(IV) and U(IV), show sulfate always in bidentate and monodentate coordination at the same time.[15,16] For U(VI), bidentate prevails over monodentate coordination at high sulfate concentrations.[17] In a solution of 1.14×10^{-2} M Pa(V) and 13 M H_2SO_4, it has been observed that three mononodentate and two bidentate sulfate groups are coordinated to Pa.[18]

Scheme 1

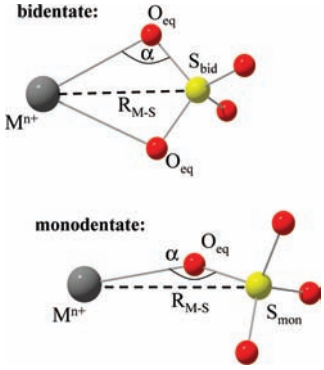

The aim of this study is to provide a systematic investigation of the aqueous sulfate complexes with neptunium in oxidation states IV, V, and VI by Np L_3-edge EXAFS spectroscopy. EXAFS is well-suited for such a kind of analysis, because sulfur has a strong backscattering power for the photoelectron wave. The obtained coordination numbers of sulfur, N_S, represent a statistical average of coexisting neptunium sulfate complexes, commonly indicative of the prevalent solution species. Significant differences occur between the metal−sulfur distances (R_{M-S}) in bidentate (bid) and monodentate (mon) sulfate coordination (see Scheme 1).

Sulfate in bidentate coordination shows a Np−S_{bid} distance of ∼3.1 Å, whereas monodentate sulfate shows a Np−S_{mon} distance of ∼3.6 Å. In the case of the monodentate coordination, there is substantial variation in the bond lengths R_{M-S}, because the angle α is more flexible than in the bidentate-chelating coordination mode. Higher flexibility of α would be indicated by an elevated Debye−Waller factor, σ^2. In principle, the two different sulfate coordinations would also be distinguishable by their typical Np−O distances, which are ∼2.3 Å for monodentate and ∼2.5 Å for bidentate coordination. However, the Np−O distance is a much weaker diagnostic tool than the Np−S distance, because the neptunium coordination polyhedron is usually comprised of different oxygen ligands from water molecules and bidentate and monodentate sulfate. The different Np−O distances are close to the resolution limit of EXAFS and contribute predominantly to the structural disorder, expressed by σ^2. Therefore, we rely in this paper solely on Np−S distances to determine sulfate coordination modes.

Experimental Section

Caution! *^{237}Np is a radioactive isotope and an α-emitter. It has to be handled in dedicated facilities with appropriate equipment for radioactive materials to avoid health risks caused by radiation exposure.*

Sample Preparation. A stock solution of 0.05 M Np(VI) in 1.0 M $HClO_4$ was prepared from neptunium (^{237}Np) dioxide (CEA-Marcoule, France) as previously described.[19] Sample solutions used for electrochemical experiments (i.e., cyclic voltammetry and bulk electrolysis) were prepared by evaporating an appropriate amount of the Np stock solution and dissolving

(6) Sulivan, J. C.; Hindman, J. C. *J. Am. Chem. Soc.* **1954**, *77*, 5931.
(7) Xia, Y.; Rao, L.; Rai, D.; Felmy, R. *Radiochim. Acta* **1999**, *86*, 33.
(8) Bolvin, H.; Wahlgren, U.; Gropen, O.; Marsden, C. *J. Phys. Chem. A* **2001**, *105*, 10570.
(9) Bolvin, H.; Wahlgren, U.; Moll, H.; Reich, T.; Geipel, G.; Fanghänel, T.; Grenthe, I. *J. Phys. Chem. A* **2001**, *105*, 11441.
(10) Williams, C. W.; Blaudeau, J.-P.; Sullivan, J. C.; Antonio, M. R.; Bursten, B.; Soderholm, L *J. Am. Chem. Soc.* **2001**, *123*, 4346.
(11) Steele, H.; Taylor, R. *Inorg. Chem.* **2007**, *46*, 6311.
(12) Hennig, C.; Servaes, K.; Nockemann, P.; Van Hecke, K.; Van Meervelt, L.; Wouters, J.; Fluyt, L.; Görrler-Walrand, C.; Van Deun, R. *Inorg. Chem.* **2008**, *47*, 6311.
(13) Antonio, M. R.; Soderholm, L. X-ray absorption spectroscopy of the actinides. In *The Chemistry of the Actinide and Transactinide Elements*; Morss, L. R., Edelstein, N. M.; Fuger, J., Eds.; Springer: New York, **2005**, Vol. 5, p 3086
(14) Reich, T.; Bernhard, G.; Geipel, G.; Funke, H.; Hennig, C. Rossberg, A.; Matz, W.; Schell, N.; Nitsche, H. *Radiochim. Acta* **2000**, *88*, 633.
(15) Hennig, C.; Schmeide, K.; Brendler, V.; Moll, H.; Tsushima, S.; Scheinost, A. C. *Inorg. Chem.* **2007**, *46*, 5882.
(16) Hennig, C.; Kraus, W.; Emmerling, F.; Ikeda, A.; Scheinost, A. C. *Inorg. Chem.* **2008**, *47*, 1634.
(17) Hennig, C.; Ikeda, A.; Schmeide, K.; Brendler, V.; Moll, H.; Tsushima, S.; Scheinost, A. C.; Skanthakumar, S.; Wilson, R.; Soderholm, L.; Servaes, K.; Görrler-Walrand, C.; Van Deun, R. *Radiochim. Acta* **2008**, *96*, 607.
(18) Le Naour, C.; Trubert, D.; Di Giandomenico, V. M.; Fillaux, C.; Den Auwer, C.; Moisy, P.; Hennig, C. *Inorg. Chem.* **2005**, *44*, 9542.
(19) Ikeda-Ohno, A.; Hennig, C.; Rossberg, A.; Funke, H.; Scheinost, A. C.; Bernhard, G.; Yaita, T. *Inorg. Chem.* **2008**, *47*, 8294.

Table 1. Sample Summary

sample ID	[Np] M	ox. state	pH	medium	preparation[a]
Np^{VI}-1	0.05	VI	1.1	0.05 M $(NH_4)_2SO_4$	dissolution[b]
Np^{VI}-2	0.05	VI	1.2	2.0 M $(NH_4)_2SO_4$	dissolution[b]
Np^{VI}-3	0.05	VI	2.7	2.0 M $(NH_4)_2SO_4$	dissolution[b]
Np^{V}-1	0.05	V	1.1	0.05 M $(NH_4)_2SO_4$	reduction of Np(VI) (= Np^{VI}-1) at 0.0 V
Np^{V}-2	0.05	V	2.7	2.0 M $(NH_4)_2SO_4$	reduction of Np(VI) (= Np^{VI}-3) at 0.1 V
Np^{IV}-1	0.04	IV	< 0.1	1.0 M $HClO_4$	reduction of Np(V) at −0.3 V
Np^{IV}-2	0.05	IV	1.1	0.5 M $(NH_4)_2SO_4$	mixing[c]
Np^{IV}-3	0.05	IV	1.1	1.0 M $(NH_4)_2SO_4$	mixing[c]
Np^{IV}-4	0.05	IV	1.1	2.0 M $(NH_4)_2SO_4$	mixing[c]
Np^{IV}-5	0.05	IV	1.1	3.0 M $(NH_4)_2SO_4$	mixing[c]

[a] Potentials for the electrolysis are referred to Ag/AgCl in 3 M NaCl. [b] Dissolution of the dried Np(VI) stock solution. [c] Mixing Np(IV)−$HClO_4$ solution with $(NH_4)_2SO_4$ solution.

the dried material into a desired composition of aqueous $(NH_4)_2SO_4$ solution. The pH of the sample solutions was adjusted by adding $HClO_4$. The concentration of Np in the sample solutions was confirmed by UV−vis−NIR absorption and α and γ spectroscopy. All other chemicals used in this study were supplied by Merck KGaA and were reagent-grade.

Electrochemical Experiments. Cyclic voltammograms of 0.05 M Np(VI) in aqueous $(NH_4)_2SO_4$ solution were recorded at 295 K using an Autolab PGSTAT302 potentiostat/galvanostat (Eco Chemie B.V.) under a N_2 atmosphere. A three-electrode system consisting of a Au working electrode (surface area = 2 mm^2), a Pt-wire counter electrode, and a Ag/AgCl reference electrode in 3.0 M NaCl were employed with a Vycor glass liquid junction. Sample solutions were deoxygenated by bubbling N_2 gas prior to the measurement. For each solution, a blank was recorded and is subtracted from the voltammogram of neptunium sulfate. On the basis of redox potentials obtained from the cyclic voltammograms, bulk electrolysis was performed to adjust the oxidation state of Np. Coulometric electrolysis of 0.05 M Np was carried out with the same potentiostat/galvanostat as used for cyclic voltammetry. The electrolysis cell was composed of Pt-mesh working and counterelectrodes and a Ag/AgCl reference electrode. The oxidation state and concentration of Np in the electrolyzed solutions were checked by UV−vis−NIR absorption spectroscopy (see Figure S2 in Supporting Information).

EXAFS Samples. Np(VI) samples were prepared by evaporating the Np stock solution and dissolving the dried material into a sulfate solution. Np(V) samples were obtained by bulk electrolysis of the corresponding Np(VI) solutions at appropriate reduction potentials. Table 1 compiles the relevant preparation conditions.

Np(IV) samples were obtained by electroreduction of the Np(VI) stock solution, subsequent mixing of Np(IV) in $HClO_4$,[19] and the use of an appropriate amount of $(NH_4)_2SO_4$ solution. The solutions were composed of 0.04−0.05 M Np and had a $[SO_4^{2-}]$ from 0.5 to 3.0 M. The samples were placed in triply sealed polystyrene/polymethyl methacrylate cuvettes with an optical path length of 10 mm. Neptunium may be susceptible to photoreactions in the X-ray beam. Therefore, we always checked the oxidation state before and after the EXAFS measurements with UV−vis−NIR absorption spectroscopy. Neither a photo-oxidation of Np(IV)[20] nor a photoreduction of Np(V)[21] were observed in our study.

EXAFS Measurements. EXAFS measurements were carried out at the Rossendorf Beamline[22] at the European Synchrotron Radiation Facility. A Si(111) double-crystal monochromator was used in the channel-cut mode. Higher harmonics were rejected by two Pt-coated mirrors. Constant beam intensity was achieved with the MOSTAB feedback control system by tuning the second monochromator crystal with a piezo device. The spectra were collected in the transmission mode using argon-filled ionization chambers for I_1 and I_2 and a mixture of 25% Ar and 75% N_2 in I_0. Across the EXAFS region, data points were collected with equidistant k steps of 0.05 $Å^{-1}$. Energy calibration of the EXAFS spectra was performed by simultaneous measurement of a Y metal foil (first inflection point at 17 038 eV). All experiments were performed at 295 K. The EXAFS oscillations were extracted from the raw absorption spectra by standard methods including a μ_0 spline approximation for the atomic background using either WinXAS[23] or EXAFSPAK[24] software. A square window function was applied for the Fourier transform (FT). The FT peaks are shifted to lower values, $R + \Delta$, relative to the true near-neighbor distances R due to the phase shift of the electron wave in the adjacent atomic potentials. This Δ shift is considered a variable during the shell fits. The EXAFS data were fitted using theoretical phase and amplitude functions calculated with the FEFF 8.20 code of Rehr and Albers.[25] The single scattering and multiple scattering (MS) paths were calculated on the basis of the crystal structure data of $Cs_2NpO_2(SO_4)_2$ for Np(VI),[26] $Na_3NpO_2(SO_4)_2(H_2O)_{2.5}$ for Np(V),[27,28] and $Cs_2Np(SO_4)_3(H_2O)_2$ for Np(IV).[29,30] Taking into account the individual noise levels at higher k values, data analysis was restricted to the k range 3.2−16.8 $Å^{-1}$ for Np(V) and Np(VI) and to 2.5−16.2 $Å^{-1}$ for Np(IV). The distance resolution ΔR, that is, the ability to differentiate neighboring atom shells in the EXAFS spectrum, is given by $\Delta R = \pi/2\Delta k$, where Δk is the k range of the spectra. Thus, ΔR is 0.12 Å for Np(V) and Np(VI) and 0.11 Å for Np(IV). Small residual peaks in the FT below $R + \Delta < 1.2$ Å are typical FT truncation artifacts and are not structural features. The amplitude reduction factor, S_0^2, was defined as 0.9 in the data fits. The threshold energy, $E_{k=0}$, was defined at 17 625 eV, regardless of the Np oxidation state, and varied as a global fit parameter, resulting in the energy shift $\Delta E_{k=0}$. The freely fitted

(20) Denecke, M. A.; Dardenne, K.; Marquardt, C. M. *Talanta* **2005**, *65*, 1008.
(21) Skanthakumar, S.; Gorman-Levis, D.; Locock, A.; Chiang, M.-H.; Jensen, M. P.; Burns, P. C.; Fein, J.; Jonah, C. D.; Attenkofer, K.; Soderholm, L. *Mater. Res. Soc. Symp. Proc.* **2004**, *802*, 151.
(22) Matz, W.; Schell, N.; Bernhard, G.; Prokert, F.; Reich, T.; Claussner, J.; Oehme, W.; Schlenk, R.; Dienel, S.; Funke, H.; Eichhorn, F.; Betzl, M.; Pröhl, D.; Strauch, U.; Huttig, G.; Krug, H.; Neumann, W.; Brendler, V.; Reichel, P.; Denecke, M. A.; Nitsche, H. *J. Synchrotron. Radiat.* **1999**, *6*, 1076.
(23) Ressler, T. *J. Synchrotron. Radiat.* **1998**, *5*, 118.
(24) George, G. N.; Pickering, I. J. *EXAFSPAK*; Stanford: Palo Alto, CA, **2000**.
(25) Rehr, J. J.; Albers, R. C. *Rev. Modern Phys.* **2000**, *72*, 621.
(26) Fedoseev, A. M.; Budantseva, N. A.; Grigoriev, M. S.; Bessonov, A. A.; Astafurova, L. N.; Lapitskaya, T. S.; Krupa, J. C. *Radiochim. Acta* **1999**, *86*, 17.
(27) Forbes, T. Z.; Burns, P. C. *J. Solid State Chem.* **2005**, *178*, 3445.
(28) Forbes, T. Z.; Burns, P. C. *Chem. Mater.* **2006**, *18*, 1643.
(29) Charushnikova, I. A.; Krot, N. N.; Starikova, Z. A. *Radiochemistry* **2000**, *42*, 42.
(30) Charushnikova, I. A.; Krot, N. N.; Polyakova, I. N. *Krystalografiya* **2006**, *51*, 231.

energy shift was linked for all shells. The refined structural parameters are the coordination number N, the interatomic distance R, and the Debye−Waller factor σ^2. The overall goodness of the fits, F, is given by χ^2 weighted by the magnitude of the data.[24] Additionally, the XANES spectra are given in Figure S3a−c of the Supporting Information.

Quantum Chemical Calculations. Calculations were performed with the Gaussian 03[31] and Molcas 7.0[32] programs. A critical point for the calculation of aqueous actinide species is a proper treatment of the solvent.[33] In this study, geometry optimization and successive vibrational frequency calculations were performed in the aqueous phase using Gaussian 03 at the restricted and unrestricted B3LYP levels through the use of the conductor-like polarizable continuum model (CPCM)[34] using UAHF radii,[35] as implemented in Gaussian 03. A small core effective core potential (SCECP) was used for thorium, neptunium, sulfur, and oxygen, comprising 60, 60, 10, and 2 electrons in the core, respectively, with corresponding basis sets.[36] The most diffuse basis functions of neptunium with the exponent 0.005 were omitted, and d functions of sulfur and oxygen bases were included. For hydrogen, a 5s contracted to a 3s basis set was used.[37] Gibbs energy was calculated, like in various recent studies,[38] through vibrational frequency calculations in the aqueous phase and by using the pressure and temperature parameters $p = 1$ atm and $T = 298.15$ K.

In neptunium complexes, multireference effects originating from strong couplings in the bare ion occur in the systems with more than one unpaired f electron.[38] The energies calculated with any unrestricted method are unreliable for strongly multiconfigurational systems, while geometry optimization of actinide complexes using single-configurational DFT is generally thought to provide reasonable results.[39] This may not hold in systems with more than two f electrons as Np(IV) for the reasons we describe in a comment (S6 in Supporting Information). We performed multireference CASPT2 calculations using Molcas 7.0. Only the most important configurations, arising from redistributions of the electrons in the low-lying f shells, are included in the reference.

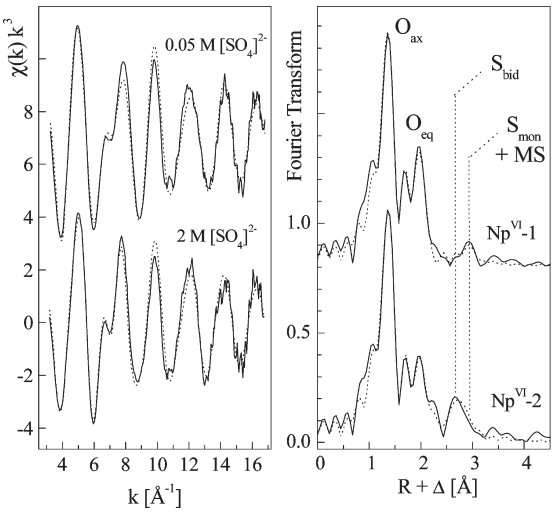

Figure 1. Np L_3-edge k^3-weighted EXAFS spectra (left) and the corresponding Fourier transforms (right) of Np(VI) sulfate species.

Results and Discussion

Np(VI) Sulfate. The L_3-edge k^3-weighted EXAFS spectra $\chi(k)$ and the corresponding FTs of Np(VI) sulfate are shown in Figure 1. The subsequent figures show the experimental EXAFS data as a solid line and the shell-fit result as a dotted line. Structure parameters of the fitting procedure including phase shift correction are summarized in Table 2.

The FT of the neptunyl(VI) ion, NpO_2^{2+}, shows a dominating peak from two axial trans-oxo atoms (O_{ax}) at a Np−O distance of 1.76 ± 0.02 Å. The equatorial shell of sample **Np^{VI}-1** exhibits five equatorial oxygen atoms (O_{eq}) at 2.41 ± 0.02 Å. A third FT peak appears between the O_{ax} and O_{eq} peaks. This peak is reproduced successfully with only the two O_{ax} and O_{eq} shells, suggesting that it arises from the superposition of these two scattering contributions. Both the Np−O_{ax} and the Np−O_{eq} distances are close to the ones determined earlier by EXAFS for the Np(VI) hydrate $[NpO_2(H_2O)_5]^{2+}$.[19,40] This is a consequence of the situation, that in equimolar $[SO_4^{2-}]$/$[NpO_2^{2+}]$ solution only one sulfate per neptunyl ion coordinates in addition to the water molecules. There occurs also a small peak at $R + \Delta \sim 3.0$ Å from multiple scattering along the $[O{=}Np{=}O]^{2+}$ moiety dominated by the 2-fold degenerated four-legged scattering path Np−O_{ax1}−Np−O_{ax2}.[41] This spectral feature was included in the curve fit by constraining its Debye−Waller factor and its effective path length to twice the values of the corresponding Np−O_{ax} single-scattering path. Nevertheless, after subtracting the MS contribution, there remains a peak at $R + \Delta \sim 3.0$ Å, which could be fitted with a sulfur atom at a distance of 3.61 Å, suggesting monodentate

(31) Frisch, M. J.; Trucks, G. W.; Schlegel, H. B.; Scuseria, G. E.; Robb, M. A.; Cheeseman, J. R.; Montgomery, J. A., Jr.; Vreven, T.; Kudin, K. N.; Burant, J. C.; Millam, J. M.; Iyengar, S. S.; Tomasi, J.; Barone, V.; Mennucci, B.; Cossi, M.; Scalmani, G.; Rega, N.; Petersson, G. A.; Nakatsuji, H.; Hada, M.; Ehara, M.; Toyota, K.; Fukuda, R.; Hasegawa, J.; Ishida, M.; Nakajima, T.; Honda, Y.; Kitao, O.; Nakai, H.; Klene, M.; Li, X.; Knox, J. E.; Hratchian, H. P.; Cross, J. B.; Bakken, V.; Adamo, C.; Jaramillo, J.; Gomperts, R.; Stratmann, R. E.; Yazyev, O.; Austin, A. J.; Cammi, R.; Pomelli, C.; Ochterski, J. W.; Ayala, P. Y.; Morokuma, K.; Voth, G. A.; Salvador, P.; Dannenberg, J. J.; Zakrzewski, V. G.; Dapprich, S.; Daniels, A. D.; Strain, M. C.; Farkas, O.; Malick, D. K.; Rabuck, A. D.; Raghavachari, K.; Foresman, J. B.; Ortiz, J. V.; Cui, Q.; Baboul, A. G.; Clifford, S.; Cioslowski, J.; Stefanov, B. B.; Liu, G.; Liashenko, A.; Piskorz, P.; Komaromi, I.; Martin, R. L.; Fox, D. J.; Keith, T.; Al-Laham, M. A.; Peng, C. Y.; Nanayakkara, A.; Challacombe, M.; Gill, P. M. W.; Johnson, B.; Chen, W.; Wong, M. W.; Gonzalez, C.; Pople, J. A. *Gaussian 03*, revision D.01; Gaussian, Inc.: Pittsburgh, PA, **2004**.

(32) Karlström, G.; Lindh, R.; Malmqvist, P. Å.; Roos, B. O.; Ryde, U.; Veryazov, V.; Widmark, P. O.; Cossi, M.; Schimmelpfennig, B.; Neogrady, P.; Seijo, L. *Comput. Mater. Sci.* **2003**, *28*, 222.

(33) (a) Gutowski, K. E.; Dixon, D. A. *J. Phys. Chem. A* **2006**, *110*, 8840. (b) Infante, I.; Visscher, L. *J. Comput. Chem.* **2004**, *25*, 386. (c) Vallet, V.; Macak, P.; Wahlgren, U.; Grenthe, I. *Theor. Chem. Acc.* **2006**, *115*, 145. (d) Buhl, M.; Kabrede, H.; Diss, R.; Wipff, G. *J. Am. Chem. Soc.* **2006**, *128*, 6357.

(34) (a) Barone, V.; Cossi, M. *J. Phys. Chem. A* **1998**, *102*, 1995. (b) Cossi, M.; Rega, N.; Scalmani, G.; Barone, V. *J. Comput. Chem.* **2003**, *24*, 669.

(35) Bondi, A. *J. Phys. Chem.* **1964**, *68*, 441.

(36) (a) Kuchle, W.; Dolg, M.; Stoll, H.; Preuss, H. *J. Chem. Phys.* **1994**, *100*, 7535. (b) Bergner, A.; Dolg, M.; Kuechle, W.; Stoll, H.; Preuss, H. *Mol. Phys.* **1993**, *80*, 1431.

(37) Krishnan, R.; Binkley, J. S.; Seeger, R.; Pople, J. A. *J. Chem. Phys.* **1980**, *72*, 650.

(38) Tsushima, S.; Wahlgren, U.; Grenthe, I. *J. Phys. Chem. A* **2006**, *110*, 9175.

(39) (a) Schlosser, F.; Kruger, S.; Rösch, N. *Inorg. Chem.* **2006**, *45*, 1480. (b) Yang, T. X.; Bursten, B. *Inorg. Chem.* **2006**, *45*, 5291. (c) Wander, M. C. F.; Kerisit, S.; Rosso, K. M.; Schoonen, M. A. A. *J. Phys. Chem. A* **2006**, *110*, 9691. (d) Tsushima, S. *J. Phys. Chem. A* **2007**, *111*, 3613. (e) Real, F.; Vallet, V.; Wahlgren, U.; Grenthe, I. *J. Am. Chem. Soc.* **2008**, *130*, 11742. (f) Shamov, G. A.; Schreckenbach, G. *J. Am. Chem. Soc.* **2008**, *130*, 13737.

(40) Antonio, M. R.; Soderholm, L.; Williams, C. W.; Blaudeau, J.-P.; Bursten, B. E. *Radiochim. Acta* **2001**, *89*, 17.

(41) Hudson, E. A.; Rehr, J. J.; Bucher, J. J. *Phys. Rev. B* **1995**, *52*, 13815.

Table 2. EXAFS Fit Parameters of Np(VI) Sulfate Species

sample	scattering path	R [Å]	N	σ^2 [Å^2]	$\Delta E_{k=0}$	F
Np^{VI}-1	Np−O_{ax}	1.76	2.0	0.0014	3.8	0.19
	Np−O_{eq}	2.41	5.1	0.0053		
	Np−S_{bid}	3.12	< 0.2	0.006[a]		
	Np−S_{mon}	3.61	< 0.4	0.009[a]		
Np^{VI}-2	Np−O_{ax}	1.76	1.9	0.0014	4.3	0.21
	Np−$O_{eq\ 1}$	2.34	1.4	0.0071		
	Np−$O_{eq\ 2}$	2.48	3.4	0.0078		
	Np−S_{bid}	3.13	1.8	0.006[a]		
	Np−S_{mon}	3.60	< 0.4	0.009[a]		
Np^{VI}-3	Np−O_{ax}	1.76	1.9	0.0013	4.6	0.22
	Np−$O_{eq\ 1}$	2.34	1.2	0.0069		
	Np−$O_{eq\ 2}$	2.51	3.8	0.0079		
	Np−S_{bid}	3.13	2.1	0.006[a]		
	Np−S_{mon}	3.62	< 0.3	0.009[a]		

[a] Value fixed during the fit procedure. Errors in distances are ±0.02 Å; errors in coordination numbers are ±15%.

coordinated sulfate. An additional peak could be fitted with sulfur at a distance of 3.12 Å, which would be in line with bidentate sulfate coordination. While the intensity of this peak is close to the noise level at a low sulfate concentration, it increases with sulfate concentration, suggesting a real backscattering effect. In sample **Np^{VI}-2** with 2.0 M SO_4^{2-}, there are approximately two sulfate atoms per neptunyl unit present. The data indicate that the coordination mode changes with increasing sulfate concentration from a prevalent monodentate to a prevalent bidentate coordination. The same tendency has been observed for U(VI) sulfate in aqueous solution. For solutions with low $[SO_4^{2-}]/[UO_2^{2+}]$ ratios, monodentate sulfate coordination has been observed with infrared spectroscopy,[42] high-energy X-ray scattering (HEXS),[43] and EXAFS.[15] In contrast, in solutions with high $[SO_4^{2-}]/[UO_2^{2+}]$ ratios, the dominance of bidentate coordinated sulfate has been confirmed by Raman,[44] HEXS,[17] and EXAFS.[15,45] The change in the U(VI) sulfate coordination mode is hence a function of the $[SO_4^{2-}]/[UO_2^{2+}]$ ratio. The Np(VI) sulfate species shows the same behavior.

The structure of possible Np(VI) sulfate species was investigated by DFT calculations. Three complexes were studied, which are assumed to represent dominating species, namely, NpO_2SO_4(aq) in bidentate (Figure 2a) and monodentate (Figure 2b) coordination and $NpO_2(SO_4)_2^{2-}$ in bidentate coordination (Figure 2c). Their structures and the major distances between Np and the ligand atoms are given in Figure 2.

The Np−O and Np−S distances in the complexes obtained by DFT calculations are similar to those of the corresponding U(VI) sulfate complexes.[15] For example, Np−S distances in NpO_2SO_4(aq) are 3.06 and 3.68 Å, and in $NpO_2(SO_4)_2^{2-}$ is 3.08 Å, while U−S distances in corresponding U(VI) complexes are 3.69 and 3.08 Å. The EXAFS-derived atomic distances of corresponding U and Np complexes deviate from the DFT results. For

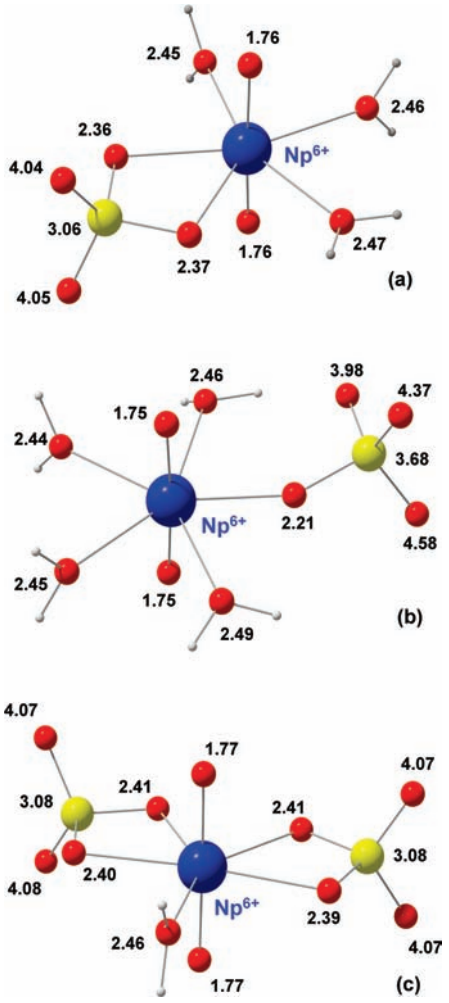

Figure 2. Structures of NpO_2SO_4(aq) (a,b) and $NpO_2(SO_4)_2^{2-}$ (c), obtained by DFT calculations in the aqueous phase (SCECP-B3LYP-CPCM). Distances between neptunium and the ligand atoms are given in ångstroms.

example, U−S_{mon} distances are 3.56−3.58 Å, and the Np−S_{mon} distances are 3.60−3.62 Å. The origin of the discrepancy and its trend opposite of the commonly observed contraction along the actinide series is not clear for the moment but is perhaps related to the coordination outside the sulfate ligand, that is, hydrogen-bond and counterion interaction with sulfate oxygen. A similar tendency was previously observed for neptunium nitrate.[19] For comparison, it should be mentioned that, for aqueous solution, the UO_2SO_4(aq) and $UO_2(SO_4)_2^{2-}$ complex could be identified, but not the $UO_2(SO_4)_3^{4-}$ complex. Even at high temperatures, only the $UO_2(SO_4)_2^{2-}$ complex has been observed.[46] The $UO_2(SO_4)_3^{4-}$ species occurs obviously only in solutions with a very high sulfate excess.[47,48] Np(VI) behaves in the same sense as U(VI) with respect to changes in the sulfate coordination mode. Two isomers can be observed for the species NpO_2SO_4(aq), one with the sulfate in monodentate coordination

(42) Gál, M.; Goggin, P. L.; Mink, J. *Spectrochim. Acta A* **1992**, *48*, 121.
(43) Neuefeind, J.; Skanthakumar, S.; Soderholm, L. *Inorg. Chem.* **2004**, *43*, 2422.
(44) Nguyen-Trung, C.; Begun, G. M.; Palmer, D. A. *Inorg. Chem.* **1992**, *31*, 5280.
(45) Moll, H.; Reich, T.; Hennig, C.; Rossberg, A.; Szabó, Z.; Grenthe, I. *Radiochim. Acta* **2000**, *88*, 559.
(46) (a) Rao, L.; Tian, G. *Uranium, Mining and Hydrogeology*; Springer: Heidelberg, Germany, **2008**; p 763.(b) Tian, G.; Rao, L. *J. Chem. Thermodynamics* **2009**, *41*, 569.
(47) Geipel, G.; Brachmann, A.; Brendler, V.; Bernhard, G.; Nitsche, H. *Radiochim. Acta* **1996**, *75*, 199.
(48) Vercouter, T.; Vitorge, P.; Amekraz, B.; Moulin, C. *Inorg. Chem.* **2008**, *47*, 2180.

and one with the sulfate in bidentate coordination. For $NpO_2(SO_4)_2^{2-}$, the bidentate coordination prevails. This result is in agreement with our former observations on U(VI) sulfate species.[15,17]

Np(V) Sulfate. Np(V) sulfate has no uranium counterpart, because U(V) rapidly disproportionates to U(IV) and U(VI). Np(V) forms usually only weak complexes, and the revised formation constant is reported only for the sulfate species $NpO_2SO_4^-$.[5,49,50] The L_3-edge k^3-weighted EXAFS data of Np(V) with 0.05 and 2.0 M SO_4^{2-} are shown in Figure 3, and the fit parameters are given in Table 3.

The trans-dioxo structure remains intact, but the charge is reduced in comparison to Np(VI). Np(VI) and Np(V) have formal electronic configurations of $5f^1$ and $5f^2$, respectively. The additional electron occupies mainly the nonbonding 5fϕ or 5fδ orbitals of Np(V)[38] and is localized mainly on the Np atom. Therefore, the effective charge of the central atom in Np(V) is smaller compared to that of Np(VI), and both the axial and equatorial Np−O distances are longer than those of Np(VI). This is confirmed by the DFT calculations, indicating that the $Np-O_{ax}$ and $Np-O_{eq}$ distances of Np(V) are approximately 0.05 and 0.10 Å longer than those of Np(VI). On the basis of EXAFS spectroscopy, we derived two isomers for the species $NpO_2SO_4^-$ with sulfate either in monodentate or in bidentate coordination. These isomers are depicted in Figure 4 together with the distances between neptunium and the ligand atoms obtained by the DFT calculations.

The EXAFS data show a $Np-O_{ax}$ distance of 1.83 Å in Np(V) sulfate. Within the typical error limits, this is the same distance as in Np(V) hydrate.[19,40,51,52] Similarly, the equatorial oxygen distances of Np(V) sulfate and hydrate are identical. The sulfate coordination of Np(V) is less pronounced than that of Np(VI), even at high sulfate concentrations. Less than 0.4 monodentate sulfate groups at a $Np-S_{mon}$ distance of 3.67 Å were observed with 0.05 M SO_4^{2-}. The small sulfate coordination number suggests that the hydrate remains dominant under these experimental conditions. By raising the sulfate concentration to 2.0 M, a change in the sulfate coordination can be observed: an additional small peak indicates the presence of bidentate sulfate with a $Np-S_{bid}$ distance of 3.16 Å. The corresponding coordination number is only 0.5. The combined coordination number of monodentate and bidentate sulfate does not exceed one sulfate per Np(V) ion. A higher sulfate coordination as in the species $NpO_2(SO_4)_2^{3-}$ has been observed in solutions with pH > 5 and an elevated temperature.[53] It should be mentioned that also in crystal structures Np(V) sulfate is observed in the monodentate and bidentate sulfate coordination modes. Most of these crystal structures show a coordination number of five oxygen atoms in the equatorial plane,[28,30] and similar Np−S bond lengths to those observed in solution. There also exist crystal structures with a six-fold equatorial coordination. However, the Np−S distances in the six-fold structure are significantly longer: the distance $Np-S_{bid}$ is 3.22−3.25 Å, and the distance $Np-S_{mon}$ is 3.80−3.84 Å.[27] The shorter Np−S distances observed in the solutions described here are an additional indicator for an equatorial coordination number of five. In comparison to EXAFS, the $Np-S_{bid}$ distance obtained by DFT is slightly underestimated, while it is known that the SCECP-B3LYP-CPCM method tends to overestimate the An−O bonds.[54] The $Np-S_{mon}$ distance exhibits a larger discrepancy between EXAFS (3.67 Å, Table 3) and DFT (3.81 Å, Figure 4). This may be attributed to the angular flexibility of the monodentate arrangement, which is not as rigid as that of the bidentate complex. Therefore, the angle may easily change with the orientation of water molecules in the second shell and the counterions. This is more likely to be the case for Np(V) because the metal−ligand interaction is much weaker than that in the corresponding Np(VI) complexes.

The redox reaction between Np(V) and Np(VI) is regarded as a one-electron transfer reaction according to

$$Np^{V}O_2^+ \leftrightarrow Np^{VI}O_2^{2+} + e^- \quad (1)$$

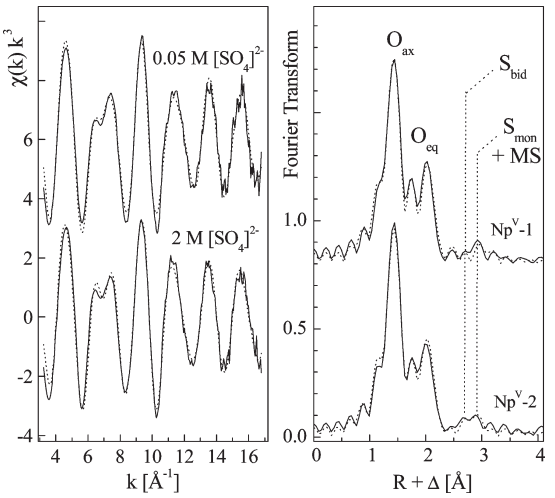

Figure 3. Np L_3-edge k^3-weighted EXAFS spectra (left) and the corresponding Fourier transforms (right) of Np(V) sulfate species.

Table 3. EXAFS Fit Parameters of Np(V) Sulfate Species

sample	scattering path	R [Å]	N	σ^2 [Å^2]	$\Delta E_{k=0}$	F
Np^V-1	$Np-O_{ax}$	1.83	2.0	0.0015	0.3	0.19
	$Np-O_{eq}$	2.50	4.6	0.0066		
	$Np-S_{mon}$	3.67	< 0.4	0.009[a]		
Np^V-2	$Np-O_{ax}$	1.83	1.9	0.0014	−1.5	0.20
	$Np-O_{eq}$	2.50	4.7	0.0078		
	$Np-S_{bid}$	3.16	0.5	0.006[a]		
	$Np-S_{mon}$	3.67	< 0.3	0.009[a]		

[a] Value fixed during the fit procedure. Errors in distances are ±0.02 Å; errors in coordination numbers are ±15%.

(49) Halperin, J.; Oliver, J. J. *Radiochim. Acta* **1983**, *33*, 29.
(50) (a) Rao, L; Tian, G.; Xia, Y. Friese, J. I. *Proc. 11th Int. High-Level Radioactive Waste Management Conf.*, Las Vegas, April 30−May 4, **2006**; pp 374−378.(b) Rao, L; Tian, G.; Xia, Y.; Friese, J. I. *J. Therm. Anal. Cal.* **2009**, *95*, 409.
(51) Allen, P. G.; Bucher, J. J.; Shuh, D. K.; Edelstein, N. M.; Reich, T. *Inorg. Chem.* **1997**, *36*, 4676.
(52) Den Auwer, C.; Simoni, E.; Conradson, S.; Madic, C. *Eur. J. Inorg. Chem.* **2003**, 3843.
(53) Xia, Y.; Friese, J. I.; Moore, D. A.; Rao, L. *J. Radioanal. Nucl. Chem.* **2006**, *268*, 445.
(54) Shamov, G. A.; Schreckenbach, G. *J. Phys. Chem. A* **2005**, *109*, 10961.

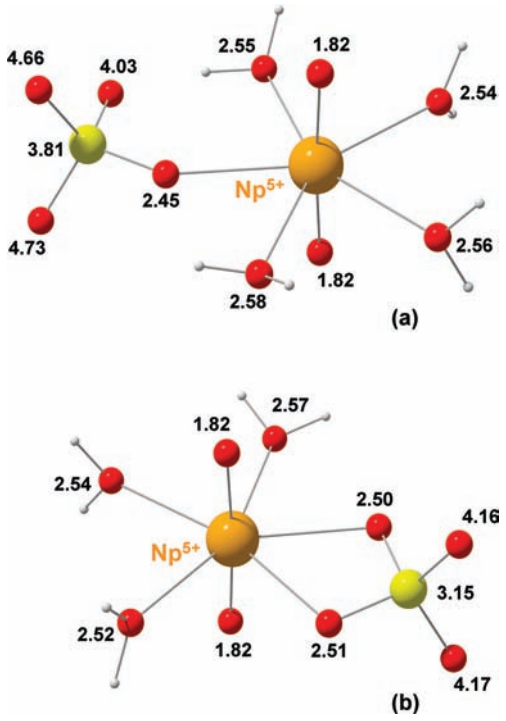

Figure 4. Structures obtained by DFT calculations in the aqueous phase (SCECP-B3LYP-CPCM). $NpO_2SO_4^-$ with monodentate (a) and bidentate (b) sulfate coordination. Distances between neptunium and the ligand atoms are given in ångstroms.

In noncomplexing media like $HClO_4$ or $[HNO_3]$ at <1 M, this reaction is reversible or at least quasi-reversible.[19,55−57] The reason might be that either the one-electron redox reaction is not influenced by the change in hydration number or the hydration number remains unchanged, as indicated by EXAFS data.[19] Because the number of sulfates coordinated by Np(VI) and Np(V) is significantly different, the question rises, whether the electrode kinetics are influenced by a change of the sulfate coordination. For this purpose, solutions with low and high sulfate concentrations were investigated. Figure 5 shows the cyclic voltammograms of 0.05 M Np(VI) in 0.05 M and in 2.0 M $(NH_4)_2SO_4$ at pH 1.1.

The Np(VI)/Np(V) redox peak at ~1.0 V is quasi-reversible in 0.05 M SO_4^{2-}, but it becomes evidently more irreversible in 2.0 M SO_4^{2-}. To verify the degree of reversibility of the Np(VI)/Np(V) redox couple, cyclic voltammetry measurements with different scan rates were carried out (Figure S4 of the Supporting Information). In an ideal reversible system, the scan rate has no influence on the anodic/cathodic wave separation. The potential difference between anodic and cathodic peaks ($|E_{Pa} - E_{Pc}|$) increases with increasing scan rate, as shown in Figure S4. The difference $|E_{Pa} - E_{Pc}|$ is more enhanced at higher SO_4^{2-} concentrations, indicating that the redox reaction between the Np(VI)/Np(V) couple approaches an irreversible state.

A further reduction results in a second redox couple at −0.3 V. The reduction of Np(V) to Np(IV) requires the release of the two axial oxygen atoms of NpO_2^+. This reaction is kinetically hindered and happens to be irreversible because the electrode reaction is slow due to the formation or breakage of the actinyl bonds.[58−60] Because the $E_{1/2}$ values of Np(V)/Np(IV) and Np(IV)/Np(III) are only separated from each other by ~0.2 V,[59,61] a superposition of the redox reactions results:

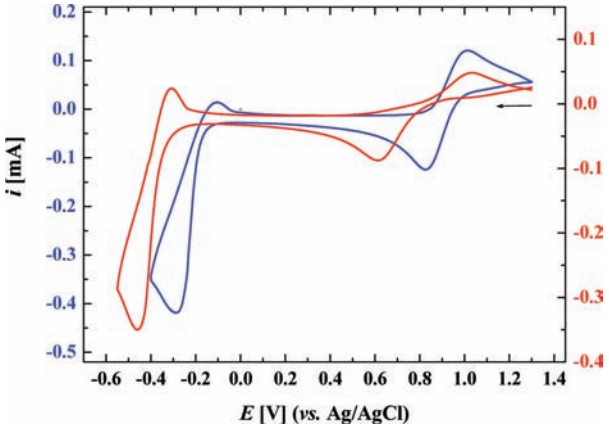

Figure 5. Cyclic voltammograms of 0.05 M Np(VI) in 0.05 M (blue line) and 2.0 M $(NH_4)_2SO_4$ (red line) at pH 1.1. Au working electrode; start potential, 1.3 V; initial scan direction, cathodic; scan rate, 400 mV/s.

$$NpO_2^+ + 4H^+ + e^- \leftrightarrow Np^{4+} + 2H_2O \qquad (2)$$

and

$$Np^{4+} + e^- \leftrightarrow Np^{3+} \qquad (3)$$

This two-electron transfer reaction can be deduced from the larger current amplitude of the cathodic wave in Figure 5 or quantitatively from coulopotentiograms.[62] The corresponding oxidation peak in the cyclic voltammogram is weaker, probably because the reduction of Np(IV) to Np(III) is incomplete due to a competition of generated H^+ and a fast reoxidation of Np(III) in the bulk solution, reducing the amount of Np(III) present at the electrode surface. Increasing sulfate concentration results in a negative shift of the redox potentials.

The observation that the redox couple Np(VI)/Np(V) becomes irreversible with an increase in the sulfate concentration needs an explanation. Because both NpO_2^{2+} and NpO_2^+ keep their dioxo moiety unchanged, the only possibility to influence the electron transfer kinetics is a rearrangement in the inner-sphere or outer-sphere coordination. The quasi-reversible character of the Np(VI)/Np(V) redox couple in the case of a low sulfate concentration can be understood as the effect of the dominant hydration sphere that is obviously not influenced by the redox reaction. To probe the differences in the coordination of Np(V) and Np(VI) at high sulfate concentrations, two samples ($\mathbf{Np^{VI}}$**-3** and $\mathbf{Np^{V}}$**-2**) were prepared by electrolysis in 2.0 M $(NH_4)_2SO_4$ at a pH of 2.7. The pH was

(55) Niese, U.; Vecernik, J. *Isotopenpraxis* **1982**, *18*, 191.
(56) Yamamura, T.; Watanabe, N.; Yano, T.; Shiokawa, Y. *J. Electrochem. Soc.* **2005**, *152*, A830.
(57) Kim, S.-Y.; Asakura, T.; Morita, Y. *Radiochim. Acta* **2005**, *93*, 767.
(58) Cohen, D.; Hindman, J. C. *J. Am. Chem. Soc.* **1952**, *74*, 4682.
(59) Kihara, S.; Yoshida, Z.; Aoyagi, H.; Meda, K.; Shirai, O.; Kitatsuji, Y.; Yoshida, Y. *Pure Appl. Chem.* **1999**, *71*, 1771.
(60) Casadio, S.; Orlandi, F. *J. Electroanal. Chem.* **1971**, *33*, 212.
(61) Li, Y.; Kato, Y.; Yoshida, Z. *Radiochim. Acta* **1993**, *60*, 115.
(62) Aoyagi, H.; Kitatsuji, Y.; Yoshida, Z.; Kihara, S. *Anal. Chim. Acta* **2005**, *538*, 283.

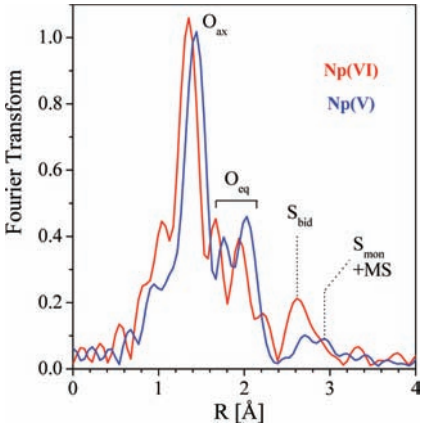

Figure 6. Comparison of the Np L_3-edge EXAFS FTs of Np(VI) and Np(V) sulfate species in 2.0 M $(NH_4)_2SO_4$ at pH 2.7.

increased in order to reduce the potential influence of the hydrated ion. These samples represent similar oxidized and reduced neptunium species that are supposed to be present at the electrode surface during cyclic voltammetry. The FTs of the corresponding EXAFS spectra are shown in Figure 6 and the data fit in Tables 2 (**Np^{VI}-3**) and 3 (**Np^{V}-2**).

Figure 6 shows the elongation of distances for Np(V) in comparison to Np(VI), as already discussed in the previous section. Similar peak heights in both spectra suggest that the coordination number of monodentate sulfate remains more or less the same. In contrast, the coordination number of bidentate sulfate is reduced from 2.1 for Np(VI) to 0.5 for Np(V). This indicates a significant rearrangement in the coordination shell during the Np(VI)/Np(V) redox reaction, which may be the reason for the kinetic hindrance of the electron transfer from the neptunium ion to the electrode. Therefore, the irreversible character of the Np(VI)/Np(V) redox couple in the sample with 2.0 M SO_4^{2-} can be regarded as a consequence of rearrangement in the sulfate coordination.

Np(IV) Sulfate. To avoid the spontaneous oxidation of Np(IV) by water[13] according to

$$Np^{4+} + 2H_2O \leftrightarrow Np^{V}O_2^{+} + 4H^{+} + e^{-} \qquad (4)$$

the concentration of sulfate was always kept above 0.5 M. The interaction of Np(IV) with ions in solution results in a spherical ligand arrangement. The coordination of the Np(IV) aquo ion has been the subject of several EXAFS studies. Allen et al. observed 11.2 O atoms at an average distance of 2.40 Å without any indication of inner-sphere coordination of Cl^- ions with 5 mM Np(IV) in 1 M HCl.[51] Antonio et al. investigated a dilute solution of 4.7 mM Np(IV) in 1 M $HClO_4$ and found a coordination number of 9 (±1) oxygen neighbors from H_2O at a distance of 2.37(2) Å.[40] Our recent investigation with 40 mM Np(IV) in 1 M $HClO_4$ revealed 10.4 (±1) oxygen atoms at 2.40(1) Å.[19] The differences of the coordination numbers reflect the typical error limit of EXAFS spectroscopy. It has not been investigated up to now whether the Np(IV) hydrate comprises several aquo species, as has been discussed for $UO_2(H_2O)_n^{2+}$, with $n = 4$ and 5,[63] and

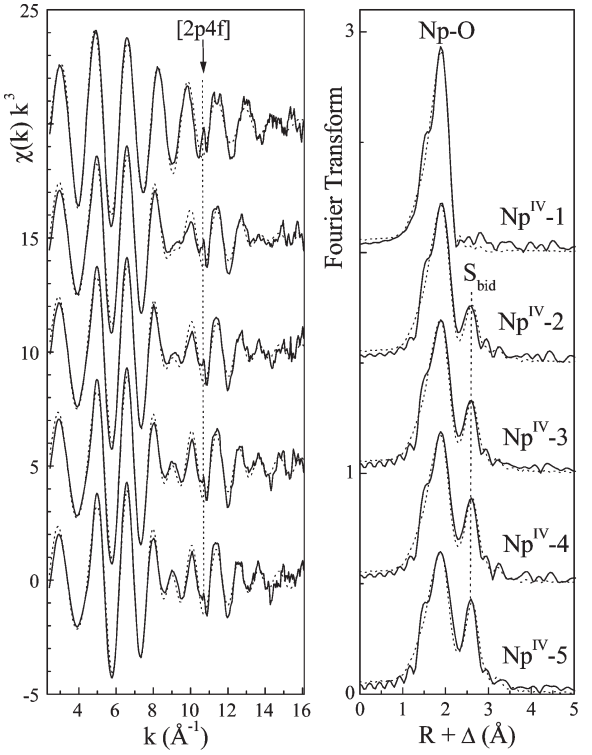

Figure 7. Np L_3-edge k^3-weighted EXAFS spectra (left) and the corresponding Fourier transforms (right) of Np(IV) sulfate species.

$Am(H_2O)_n^{3+}$, with $n = 8$ and 9.[64] However, it could be expected that the average coordination number of Np(IV) would rather increase if H_2O is replaced by bidentate chelating sulfate groups, as has been observed for several carbonate complexes.[65,66]

Figure 7 shows a series of Np(IV) sulfate samples at pH 1.1. The fit results are summarized in Table 4.

The Np(IV) hydrate (**Np^{IV}-1**) is shown for comparison. The EXAFS spectra reveal the [2p4f] double-electron excitations[67] indicated with a dotted line at $k \sim 10.7$ Å^{-1}. In the EXAFS of Np(IV), this feature appears more pronounced than in the spectra of Np(V) and Np(VI). This is related to a stronger resonance intensity due to a higher final state density. Furthermore, the $\chi(k)$'s obtained from Np(IV) solutions show weaker scattering amplitudes at high k values; hence, the double-electron excitations become more obvious. The double-electron excitation may influence to a certain extent the spline approximation and may therefore bias the related coordination numbers but will not significantly influence the interatomic distances. Most of the sulfate is coordinated in the bidentate mode with a $Np-S_{bid}$ distance of 3.07 ± 0.02 Å. Only a minor part is coordinated in the monodentate mode with a $Np-S_{mon}$ distance of 3.79 ± 0.02 Å. The sulfate coordination increases with increasing concentration, as depicted in Figure 8.

At 2.0 M $(NH_4)_2SO_4$, an average of 3.0 sulfurs bind bidentately. At the same sulfate concentration but lower

(63) Soderholm, L.; Skanthakumar, S.; Neuefeind *J. Anal. Bioanal. Chem.* **2005**, *383*, 48.

(64) Lindqvist-Reis, P.; Klenze, R.; Schubert, G.; Fanghänel, T. *J. Phys. Chem. B* **2005**, *109*, 3077.

(65) Ikeda, A.; Hennig, C.; Tsushima, S.; Takao, K.; Ikeda, Y.; Scheinost, A. C.; Bernhard, G. *Inorg. Chem.* **2007**, *46*, 4212.

(66) Clark, D. L.; Conradson, S. D.; Keogh, D. W.; Palmer, P. D.; Scott, B. L.; Tait, C. D. *Inorg. Chem.* **1998**, *37*, 2893.

(67) Hennig, C. *Phys. Rev. B* **2007**, *75*, 035120.

Table 4. EXAFS Fit Parameters of Np(IV) Sulfate Species

sample	scattering path	R [Å]	N	σ^2 [Å^2]	$\Delta E_{k=0}$	F
Np^{IV}-1	Np−O	2.39	9.5	0.0074	4.2	0.19
Np^{IV}-2	Np−O	2.39	8.7	0.0087	4.3	0.20
	Np−S_{bid}	3.06	2.0	0.0048		
	Np−S_{mon}	3.78	1.1	0.008[a]		
Np^{IV}-3	Np−O	2.39	9.1	0.0096	4.2	0.21
	Np−S_{bid}	3.06	2.4	0.0045		
	Np−S_{mon}	3.79	1.3	0.008[a]		
Np^{IV}-4	Np−O	2.39	9.1	0.0098	4.1	0.20
	Np−S_{bid}	3.07	3.0	0.0052		
	Np−S_{mon}	3.78	1.4	0.008[a]		
Np^{IV}-5	Np−O	2.39	8.9	0.011	3.7	0.21
	Np−S_{bid}	3.07	3.3	0.0049		
	Np−S_{mon}	3.79	1.4	0.008[a]		

[a] Value fixed during the fit procedure. Errors in distances are ±0.02 Å; errors in coordination numbers are ±15%.

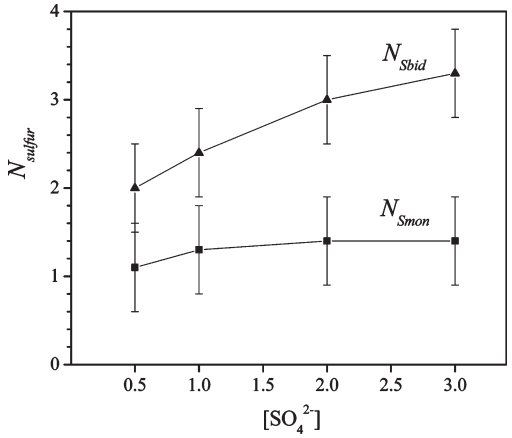

Figure 8. Coordination number of sulfur atoms as a function of the $[SO_4^{2-}]$ concentration, Np(IV) series, pH = 1.1.

pH, only 2.2 bidentate sulfate ligands were observed by Reich et al.[14] This seems to be reasonable due to the increasing influence of the aquo species with decreasing pH value. Figure 8 shows that increasing SO_4^{2-} to 3.0 M results in a further increase of bidentate coordination. The bidentate sulfate seems to replace both water and monodentate sulfate ligands. A similar trend was observed in a series of U(IV) sulfate samples under similar experimental conditions.[15] It was possible to preserve a U(IV) sulfate molecule from solution in a crystal structure, where it remained as a mononuclear complex coordinated by three bidentate sulfate, two monodentate sulfate, and one water molecule.[16] Although with increasing bidentate sulfate coordination an increase of the average oxygen coordination number would be expected, it is obvious that the FT peak intensity of the Np(IV) sulfate decreases. A clear indication of the structural change is the increasing Debye−Waller factor of the oxygen coordination shell. There is no detectable change in the average Np−O_{sul} distance for the whole series of samples. Because bidentate and monodentate sulfate coordination increases together, the longer distances of Np−O_{sul_bid} (~2.5 Å) and the shorter one of Np−O_{sul_mon} (~2.3 Å) compensate their influence on the average bond length. This shows, again, that the Np−S scattering contribution is more sensitive than that of Np−O for determining the sulfate coordination mode. A wide variety of Np(IV) sulfate species can be

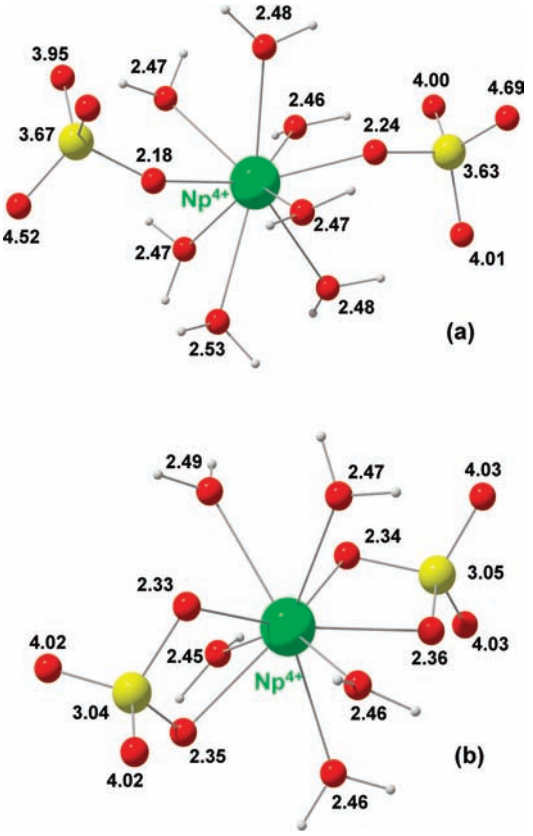

Figure 9. Structures of $Np(SO_4)_2(aq)$ obtained by DFT calculations in the aqueous phase (SCECP-B3LYP-CPCM) with sulfate in monodentate (a) and bidentate (b) coordination. Distances between neptunium and the ligand atoms are given in ångstroms.

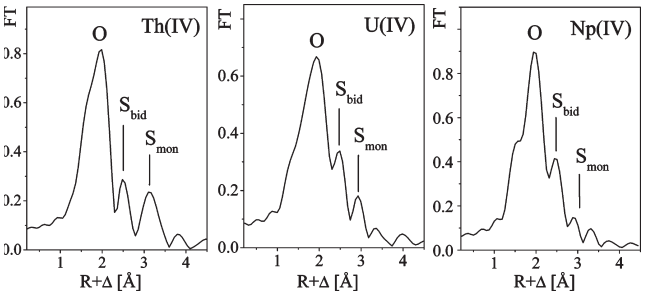

Figure 10. Comparison of the EXAFS Fourier transforms of Th(IV)/0.4 M SO_4^{2-} and U(IV)/0.4 M SO_4^{2-} taken from ref 15, with Np(IV)/0.5 M SO_4^{2-}, k = 4.2−14.1 Å.

expected from the EXAFS data. Some of these species were studied by DFT calculation. As an example, two of the possible isomers of $Np(SO_4)_2(aq)$ are given in Figure 9; some more are given in Table S5 of the Supporting Information.

It was not possible to calculate with DFT further complex species, such as $An(SO_4)_3^{2-}$ or $An(SO_4)_4^{4-}$, due to difficulties in finding energy minima. Therefore, a direct comparison of DFT results with EXAFS experiments is not possible. The data available in the recent literature for Np(IV) sulfate are not satisfactory neither with respect to the numbers of coordinated sulfate ligands nor with respect to the coordination mode of the solution species. Revised formation constants are reported only for USO_4^{2+} and $U(SO_4)_2(aq)$,[5] whereas our study reveals in addition a total of 3.1−4.7 coordinated sulfate ligands.

Table 5. Interatomic Distances (in Å), Mulliken Charge, and Relative Gibbs Energies (in kJ/mol) of $AnSO_4^{2+}$ and $An(SO_4)_2$(aq) for An = Th, Np, and Monodentate and Bidentate Coordination Modes Obtained by DFT Calculations

		$AnSO_4^{2+}$ (1:1)				$An(SO_4)_2$(aq) (1:2)			
		Th		Np		Th		Np	
		mono	bi	mono	bi	mono	bi	mono	bi
distance	An−O_{wat}[a]	2.52	2.51	2.45	2.45	2.54	2.52	2.48	2.47
	An−O_{sul}[a,b]	2.24	2.38	2.17	2.30	2.30	2.43	2.21	2.34
	An−O_{all}[a,b]	2.48	2.48	2.42	2.41	2.48	2.48	2.42	2.41
	An−S	3.65	3.07	3.59	3.01	3.73	3.13	3.65	3.05
charge	An	2.51	2.33	2.31	2.12	2.49	2.19	2.24	1.99
	O_{sul}[a,b]	−0.81	−0.71	−0.78	−0.66	−0.86	−0.75	−0.82	−0.71
energy	ΔG_{gas}[c]	0.0	−95.2	0.0	−109.1	0.0	−144.5	0.0	−173.5
	ΔG_{solv}[d]	−1169.2	−1091.5	−1233.6	−1145.5	−450.7	−362.6	−402.4	−322.6
	ΔG_{tot}[c]	0.0	−17.5	0.0	−21.0	0.0	−56.4	0.0	−93.7

[a] Averaged values. [b] Oxygen directly coordinated to Th or Np. [c] Energy relative to the monodentate complex. [d] Referring to the change in Gibbs energy when $AnSO_4^{2+}$ or $An(SO_4)_2$(aq) is transferred into water.

Furthermore, we found clear indication of monodentate and bidentate coordination modes. A number of species, which can be described with the general formula $[Np(SO_{4,bid})_x(SO_{4,mon})_y \cdot nH_2O]^{4-2x-2y}$, may exist in equilibrium. In the study presented here, we found $x = 2.0-3.3$ and $y = 1.1-1.4$. Similar solution species have been observed for U(IV) sulfate, for example, with a stoichiometry close to $[U(SO_{4,bid})_2(SO_{4,mon})_3 \cdot H_2O]^{6-}$.[16]

When the early actinides thorium, uranium, and neptunium are compared, a change in the sulfate coordination is observed. The equilibrium constant first increases in going from Th(IV) to U(IV), then decreases in going from U(IV) to Np(IV), as shown in Table S1 in the Supporting Information (sources: Langmuir and Herman[68] for thorium and Guillaumont[5b] for uranium and neptunium). However, established thermodynamic data are available only to a limited extent, and no speciation can be estimated for the present experimental samples. Furthermore, there occurs a systematic change in the coordination mode of sulfate. Figure 10 shows a comparison of the EXAFS FTs of Th(IV), U(IV), and Np (IV) sulfate obtained under similar experimental conditions. Going from Th(IV) to Np(IV), there is an increase in the bidentate sulfate coordination ($N_{Th-S} = 0.9$, $N_{U-S} = 1.5$, $N_{Th-S} = 2.0$), but vice versa there is a decrease in the monodentate sulfate coordination ($N_{Th-S} = 3.7$, $N_{U-S} = 2.5$, $N_{Th-S} = 1.1$).[15]

To study this point further, DFT calculations of Th(IV) and Np(IV) sulfate complexes were performed. $AnSO_4^{2+}$ and $An(SO_4)_2$(aq) of both monodentate and bidentate coordination were studied. It was assumed that the coordination number remains constant at 9, which seems to be a reasonable assumption according to the previous calculations.[69,70] The DFT results, interatomic distances, Mulliken charge, and relative Gibbs energies are summarized in Table 5.

For $AnSO_4^{2+}$ (the third through sixth columns in Table 5), both Th and Np seem to prefer bidentate over monodentate coordination, but the energy difference is small (17.5 (Th) and 21.0 (Np) kJ/mol). Without inclusion of the solvation energy, bidentate coordination is preferred by almost 100 kJ/mol, but after adding the solvation energy, the total energy difference decreases to about 20 kJ/mol. One or several water molecules in the first shell are moved to the second shell when going from monodentate to bidentate coordination. Consequently, the cavity of the solute becomes larger, and the solvation energy decreases. It can be concluded that the solvation energy plays a very essential role in stabilizing the monodentate complex. The energy difference of 20 kJ/mol is within the error limit of this type of calculation; hence, both monodentate and bidentate coordination seem to be equally probable for $AnSO_4^{2+}$.

For $An(SO_4)_2$(aq) (the seventh through tenth columns of Table 5), bidentate coordination is much more favored, as compared to $AnSO_4^{2+}$. In the gas phase, the bidentate coordination clearly prevails (144.5 (Th) and 173.5 (Np) kJ/mol), and even after adding solvation energy, the bidentate coordination is still favored by 56.4 (Th) and 93.7 (Np) kJ/mol. Np(IV) and Th(IV) exhibit different coordination behaviors mainly because of the difference in the electronic configuration between Np(IV) and Th(IV). Th(IV) has a formal electronic configuration of $5f^0$, while Np(IV) has $5f^3$ with three unpaired electrons contributing mainly to nonbonding 5fδ and 5fϕ orbitals. Spin densities of Np in $Np(SO_4)_2$(aq) are 3.05 and 3.06 for the monodentate and bidentate modes, respectively, supporting the idea that unpaired electrons are almost localized on the Np atom (for the discussion on the multireference character of the system and its possible effect on the reaction energy, see S6 in the Supporting Information). Consequently, electrons are more localized on the Np(IV) atom compared to Th(IV), and furthermore, Np in $NpSO_4^{2+}$ has a lower effective charge compared to Th in $ThSO_4^{2+}$. The Mulliken net charge of the central atom in $ThSO_4^{2+}$ and in $NpSO_4^{2+}$, both coordinated in a bidentate fashion, are +2.33 and +2.12, respectively (Table 5). The actinide−ligand polarization is larger for Th than for Np sulfate, and this should result in a larger solvation energy for Th sulfate. However, the An−O distances are overall shorter in Np complexes due to the actinide contraction, and the cavity of Np complexes is smaller than that of the Th complexes, which should result in a larger solvation energy for Np sulfate. These two factors compete with each other, and the resulting solvation energy is larger for Np sulfate in

(68) Langmuir, D.; Herman, J. S. *Geochim. Cosmochim. Acta* **1980**, *44*, 1733.
(69) Tsushima, S. *J. Phys. Chem. B* **2008**, *112*, 7080.
(70) Tsushima, S.; Yang, T. X. *Chem. Phys. Lett.* **2005**, *401*, 68.

$AnSO_4^{2+}$ and larger for Th sulfate in $An(SO_4)_2(aq)$. Although it was not possible to calculate An(IV) sulfate species $An(SO_4)_n^{4-2n}$ with $n > 2$, we can summarize from present DFT calculations a general trend that (1) bidentate coordination is more preferred for Np than for Th and (2) bidentate coordination is more preferred as more sulfate binds to An(IV). These findings are well in line with the EXAFS results.

Conclusion

At all three oxidation states, IV, V, and VI, neptunium is complexed by sulfate in mono- and bidentate coordination. The strongest complexes occur for Np(IV) with a sulfate coordination close to 5 in solutions at high $[SO_4^{2-}]/[Np(IV)]$ ratios. Np(VI) forms moderately strong complexes and does not exceed a total sulfate coordination number of 2 with 2.0 M SO_4^{2-}. The coordination of Np(V) sulfate is rather weak and does not exceed in total one sulfate ligand at 2.0 M SO_4^{2-}. The Np(V)/Np(IV) redox couple is irreversible under all circumstances due to the formation or destruction of the transdioxo cation NpO_2^{+}. The Np(VI)/Np(V) redox couple is quasi-reversible at low sulfate concentrations due to a dominant hydration sphere and aquo species. It becomes irreversible at high $[SO_4^{2-}]/[NpO_2^{2+}]$ ratios as a consequence of a ligand rearrangement during the redox reaction. A systematic change of the sulfate coordination mode was observed in the series Th(IV)−U(IV)−Np(IV). Within the series, monodentate sulfate coordination decreases, whereas bidentate coordination increases. According to DFT calculations, this results from several factors. First, the solvation energy stabilizes more the monodentate coordination, while the solvation energy decreases as more sulfate bonds to An (IV). Second, due to the actinide contraction, Np(IV) sulfate has a smaller cavity than Th(IV) sulfate, and hence the solvation energy plays a more important role for Np(IV). Third, due to increasing numbers of unpaired 5f electrons, electrons are more localized on the central atom for Np(IV) than for Th(IV). As a consequence, bidentate coordination becomes more likely in Np(IV) sulfate.

Acknowledgment. This work was supported by the Deutsche Forschungsgemeinschaft under Contract HE2297/2-2. The authors gratefully acknowledge generous allocation of computational time on supercomputers at The Center for Information Services and High Performance Computing (ZIH), Technische Universität Dresden, Germany.

Supporting Information Available: UV−vis−NIR absorption and XANES spectra of the samples, cyclic voltammograms with different scan rates, thermodynamic data from the recent literature, Carthesian coordinates of the investigated complex structures, and further discussion of the DFT calculation. The material is available free of charge via the Internet at http://pubs.acs.org.